

19th CIRP Conference on Modeling of Machining Operations

# Modeling of heat transfer in tool grinding for multiscale simulations

F. Wiesener<sup>a\*</sup>, B. Bergmann<sup>a</sup>, M. Wichmann<sup>a</sup>, M. Eden<sup>b,c</sup>, T. Freudenberg<sup>b</sup>, A. Schmidt<sup>b</sup>

<sup>a</sup>Institute of Production Engineering and Machine Tools (IFW), Leibniz Universität Hannover, An der Universität 2, 30823 Garbsen, Germany

<sup>b</sup>Center for Industrial Mathematics (ZeTeM) and MAPEX Center for Materials and Processes, University of Bremen, Bremen, Germany

<sup>c</sup>Department of Mathematics and Computer Science, Karlstad University, Karlstad, Sweden

\* Corresponding author. Tel.: +49 511 762 18238; fax: +49 511 762 5115. E-mail address: [wiesener@ifw.uni-hannover.de](mailto:wiesener@ifw.uni-hannover.de)

## Abstract

Tool grinding is a fundamental process step when manufacturing cylindrical cemented carbide tools. A deeper understanding of the relationship between heat generation, heat transfer and fluid dynamics is essential to optimize the application of cooling lubrication. Due to the porous structure of the grinding tool as well as the rough surfaces of tool and workpiece, this inherently leads to multiscale problems. In this paper, an approach for modeling the heat transfer between the grinding tool, the workpiece and coolant on the microscale and mesoscale is introduced, including the effective influence of the porous structure. As a basis for the simulations, experimental investigations are conducted using individual abrasive grains. A linear relationship between the single grain chip cross section and the tangential force is established with an average RMSE of 1.421 N, allowing the total heat flux to be calculated. The results are then transferred to continuous and discontinuous 2D multiscale fluid dynamic simulations in order to predict heat generation and to potentially optimize the cooling lubrication in grinding processes.

© 2023 The Authors. Published by Elsevier B.V.

This is an open access article under the CC BY-NC-ND license (<https://creativecommons.org/licenses/by-nc-nd/4.0>)

Peer review under the responsibility of the scientific committee of the 19th CIRP Conference on Modeling of Machining Operations

*Keywords:* Tool grinding; Modeling; Material removal; Multiscale simulation; Heat transfer

## 1. Introduction

For the production of geometrically defined cutting tools such as end mills or twist drills, tool grinding is a central part of the machining process. Most of the mechanical energy introduced is converted into heat. Depending on the cutting conditions, up to 85 % of the energy is transferred to the workpiece. The remaining energy is distributed between the tool, the chips and the cooling lubricant [1]. The accumulating heat flow in the workpiece is particularly critical, as it can lead to workpiece burn and thermal induced residual stresses. This reduces the usability, surface quality and dimensional accuracy of the workpiece [2]. To counter these problems, the use of cooling lubricant is essential. In addition to the removal of chips and cleaning the grinding tool, the main focus is on minimizing process temperatures [3]. A systematic supply of the cooling lubricant into the contact zone not only improves the resulting workpiece quality, but can also increase the tool life [2].

However, the fluid dynamics in connection with the heat distribution between the contact partners such as abrasive grains, the tool bond layer, the workpiece and cooling lubricant has not yet been investigated sufficiently. To study the grinding process on different scales, multiscale simulation approaches offer a promising possibility to predict thermomechanical effects. Taking into account the behavior of individual abrasive grains and the fluid dynamic of the cooling lubricant potentially optimizes the grinding process [4]. It was shown that finite element (FE) simulations are suitable to analyze the thermal behavior of CBN grains [5]. However, with a computing time of about 100 h for the simulation of a single scratching process, this method is hardly usable for simulating a real grinding process. The objective of this paper is the microscopic consideration of individual abrasive grains and their contribution to the heat generation in the grinding process. By combining material removal and fluid dynamic simulations investigations regarding the heat transfer from abrasive grains

to the bond layer and cooling lubricant are made. The knowledge gained from the microscale can later be transferred to the whole contact area of the grinding tool. First, the multiscale approach for modeling the heat transfer and grinding power is presented in chapter 2. In subsequent, experimental data for the model parameterization is collected (Section 3.2). Finally, the temperature distribution at the contact zone is investigated in multiscale simulation studies (Section 3.3).

## 2. Approach

The porous structure of grinding tools has wide implications for the heat conduction, transport and transfer in the system. From a macroscopic point, the main goal is to identify a relatively simple but accurate model describing the heat production during the grinding process as well as the heat transfer between grinding tool, cooling lubricant and workpiece. To accomplish this, the complex geometry of the grinding tool (composite of grains and polymer bonding with an additional porous structure) and the interaction with the cooling lubricant has to be accounted for.

Consequently, a framework for modeling and simulating thermomechanical effects in tool grinding on multiple scales is developed. With this approach, the heat generation at individual abrasive grains are used as a source for the heat flow from the abrasive grain to the bond layer, workpiece and cooling lubricant. By limiting the microscopically simulated area and a subsequent scaling of the results to the entire contact area, the computational effort can be significantly reduced. At the same time, the accuracy of the results is maintained by taking the microscale into account.

### 2.1 Multiscale modeling of heat transfer in tool grinding

Below the macroscopic scale, at least two distinct scales of interest exist (Figure 1). On the microscopic scale, the most important aspect is the porous structure of the grinding tool, including individual abrasive grains, as it impacts the conduction, transport and transfer of heat between the grinding tool and cooling lubricant. On the intermediate mesoscale, an effective model is used to account for the porous structure of the bond layer, but both the tool and the workpiece still show rough surfaces of different structures. These influence the boundary conditions for fluid flow and heat transfer. On the one hand, the grinding tool surface, including the surface of the bond layer, shows rather isotropic roughness patterns. In contrast, the workpiece shows a directional roughness pattern as a consequence of the material removal process [6].

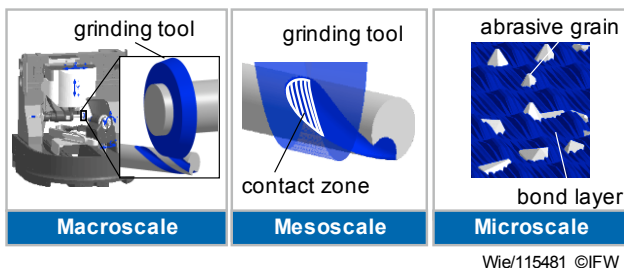


Figure 1. Multi-scale material removal simulation

Similar problems have been considered in the literature, especially with regard to free-flowing fluids interacting with saturated porous media [7, 8]. On the mesoscale, this is done by coupling the stationary Navier-Stokes system for the free-flowing lubricant with Darcy's equation for the effective movement of lubricant inside the porous medium via the Beavers-Joseph interface condition:

$$\begin{aligned} \rho_f v_f \cdot \nabla v_f &= \nabla \cdot \sigma(v_f, p_f) - g \rho_f (1 - \beta(\theta_f - \theta_0)), \\ \nabla \cdot v_f &= 0, \\ \mu K^{-1} v_p &= -\nabla p_p - g \rho_p (1 - \beta(\theta_p - \theta_0)), \\ \nabla \cdot v_p &= 0, \\ v_f \cdot n &= v_p \cdot n - M : \nabla_\tau v_f, \\ -\sigma(v_f, p_f) n \cdot n &= p_p + \eta_f n \cdot v_f + \eta_p n \cdot v_p, \\ -\sigma(v_f, p_f) n \cdot \tau &= \tau \cdot \mu K^{-\frac{1}{2}} (v_f - v_p) + \tau \cdot \mu L^{-1} v_f \end{aligned} \quad (1)$$

Here,  $\rho$  denotes densities,  $p$  pressures,  $\sigma$  the stress tensor,  $g$  the gravity,  $\beta$  the expansion coefficient,  $\mu$  the viscosity, and  $K$  the permeability matrix. Furthermore,  $\nabla_\tau$  is the gradient in tangential direction of the tangential flow,  $M$  is the transpiration length tensor,  $\eta_f, \eta_p$  are friction coefficients, and  $L$  is the effective slip length tensor [8]. While the parameters  $L$  and  $M$  can be computed from grain shapes, the friction coefficients in the effective model are identified to minimize the difference in fluid velocity and temperature to the microscale model, where the grains are modeled and a no-slip condition is applied. The temperature in the microscopic model is governed by the heat equation inside the different domains. The effective description of the heat distribution inside the porous medium depends on whether there is a local thermal equilibrium. Under the assumption of equilibrium, heat exchange between the polymer bonding and the cooling lubricant is basically instantaneous, leading to an effective model with a mixed temperature [9] :

$$\begin{aligned} \rho_f c_f (v_f \cdot \nabla \theta_f) - \kappa_f \Delta \theta_f &= 0, \\ \rho_p c_p (v_p \cdot \nabla \theta_p) - \kappa_p \Delta \theta_p &= 0, \\ -\kappa_g \Delta \theta_g &= f_s \end{aligned} \quad (2)$$

Here,  $\theta$  denotes the temperature,  $c$  the heat capacity,  $\kappa$  the heat conductivity and  $f_s$  models the heat source given via the abrasive process. The indices  $f, p, g$  indicate the free fluid, the porous medium and grains, respectively.

For the mesoscale simulations, the grain part will be removed and the porous domain extended to the height of the grains.

On the interface between grain and free fluid, different choices are possible in addition to the flux condition.

$$\kappa_f \nabla \theta_f \cdot n = \kappa_p \nabla \theta_g \cdot n, \quad (3)$$

We differentiate between the continuous model (CM), where

$$\text{CM:} \quad \theta_f = \theta_g, \quad (4)$$

and the discontinuous model (DM) with imperfect heat transmission at the interface of the form

$$\text{DM: } \kappa_f \nabla \theta_f \cdot n = \alpha (\theta_f - \theta_g) \quad (5)$$

Here,  $\alpha$  denotes the heat exchange coefficient. Similar conditions are applied at the fluid-porous and grain-porous interfaces. Corresponding (micro and meso) simulations for situations with one or more grains are presented in Section 3.3. The occurring parameters, especially on the mesoscale, later have to be determined through comparison with experimental data. In this study, for simplification, the interaction with the workpiece is neglected but will later be implemented in the model.

### 2.2 Modeling the heat generation in single grains

The mechanical energy introduced into the workpiece during the grinding process is converted into heat. Since a direct measurement of the workpiece-grain contact temperature is technologically not feasible, the contact surface-related grinding power  $P_c''$  is used as a substitute in many research studies for the evaluation of the thermomechanical load collective. Approximately this corresponds to the total heat flux [1, 10, 11]. For a helical flute grinding process, the total grinding power derives from the tangential force  $F_t$ , the cutting speed  $v_c$ , and the contact area of the tool [1, 10, 11]. To describe the heat flux  $q''$  based on a single abrasive grain on a microscopic scale, the maximum undeformed chip-cross-section of the individual grain  $A_{cu,max}$  is taken into account. This is approximated by an isosceles triangle consisting of the maximum undeformed chip thickness  $h_{cu,max}$  and the contact width of a single abrasive grain  $r_{b,max}$  [12]. In this way, the heat flow  $q''$  based on the single grain chip-cross-section  $A_{cu,max}$  can be calculated.

$$q'' = P_c'' = \frac{F_t \cdot v_c}{A_{cu,max}} = \frac{F_t \cdot v_c}{0.5 \cdot r_{b,max} \cdot h_{cu,max}} \quad (6)$$

The distribution of energy to the heat sinks grinding tool (T), cooling lubricant (F), chips (C) and workpiece (W) is obtained by taking into account the heat distribution factors  $R_i$  [11].

$$\frac{q''_T}{q''} + \frac{q''_F}{q''} + \frac{q''_C}{q''} + \frac{q''_W}{q''} = R_T + R_F + R_C + R_W = 1 \quad (7)$$

For modeling, a linear approach is developed using an empirically determined coefficient  $K_c$  for different cutting speeds. In order to scale the process to the entire grinding tool all individual grain chip-cross-sections are participating in the cutting process.

$$q_{total} = \sum_i K_c \cdot A_i(r_{b,i}, h_{cu,i}) \cdot v_c \quad (8)$$

The dixel-based simulation software IFW CutS is used, which supports a previously developed parametric grinding wheel model [6] as a digital replication of real grinding wheel topographies. The parameterization is based on the grain size, type, distribution and distance between bond layer and grain tip. In addition, the texture of the bond layer is simulated. The

advantage of this method lies in its fast and flexible application, since time-consuming topography scans are not required [6].

## 3. Experimental investigations

A central aspect of this work is the experimental determination of the coefficient  $K_c$  for modeling the grinding power at single abrasive grains. As grinding is a geometrically undefined cutting operation, the cutting conditions cannot be clearly identified due to the complex microstructure of the tool. When investigating this process in more detail, many research studies rely on single grain scratching experiments, where the movement of an individual grain is considered to be analogous to the grinding process. This approach allows investigations of the elastic and plastic material behavior [13], material removal mechanisms [14, 15], as well as thermomechanical relationships [5]. Since only a single grain is considered, deterministic results are obtained without the stochastic effects of the entire grinding tool [12].

### 3.1 Experimental setup

The setup for the single grain scratching experiments is shown in Figure 2. A surface grinding machine FS 840 KT CNC from Geibel and Hotz is used. The machine has three axes and allows the cutting depth to be set in one  $\mu\text{m}$  increments. The maximum cutting depth depends on the grinding tool used. A Kistler 9119AA2 MiniDyn dynamometer enables parallel measurement of process forces in X, Y and Z direction. The measuring system is installed in the grinding machine directly under the mounting device of the workpiece. The force components  $F_x$ ,  $F_y$  and  $F_z$  correspond to the grinding forces  $F_t$ ,  $F_a$  and  $F_n$  at the maximum depth of cut  $h_{cu,max}$ .

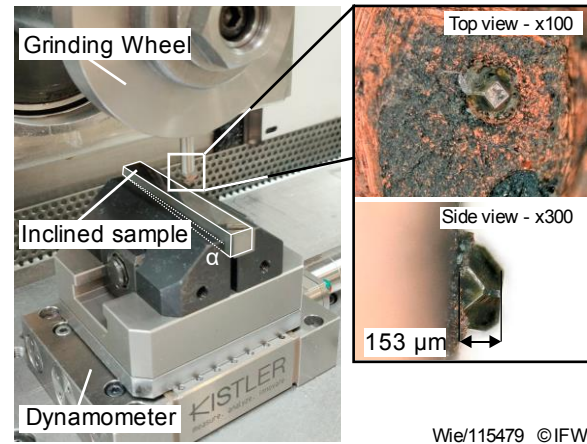


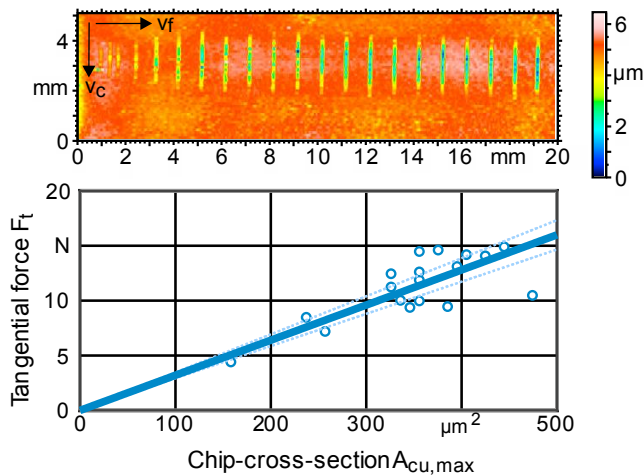
Figure 2. Experimental setup

The tool is a modified grinding wheel consisting of a steel base body, without abrasive coating. The tool includes a holder for metallic round shafts, where scratching diamonds are fixed onto the tip. The scratch diamond used in this study has a grain size of D181 (max. grain diameter 180  $\mu\text{m}$ ), surrounded by a Cr-Cu bond layer. With a total diameter of 128 mm, cutting speeds of up to 40 m/s can be reached. T10MG carbide blocks from Tigra with dimensions of 75 mm x 9 mm x 9 mm are used as the workpiece. The workpieces surface was previously polished to reduce the influence of surface roughness on the

analysis of the scratch geometry. On average, the polished areas show a roughness between  $R_z = 0.02 - 0.06 \mu\text{m}$ . The axial plunge scratching method is applied, in order to clearly assign the single grain chip-cross-sections of the individual scratches to the measured process forces. For this purpose, the sample is inclined at an angle of  $0.1^\circ$  so that the maximum single grain chip thickness  $h_{cu,max}$  increases in feed direction. Using a matching combination of cutting speed and axial feed rate, up to 15 scratches are created at an equidistant interval of 1 mm. The single grain chip thickness increases by about  $2 \mu\text{m}$  with each cut, so that the theoretically possible single grain chip thickness at the last scratch is about  $30 \mu\text{m}$ . The cutting speed is varied in three steps between 5, 10 and 20 m/s.

### 3.2 Evaluation and Results

In total a number of 37 evaluable scratches were examined in this test series. Due to the individual geometry of each grain, repeat tests with identical diamonds are not possible. For this reason, two scratch processes with similar grains and same process parameters were conducted for each experiment, resulting in scratch geometries with comparable chip cross-sections. The upper section of Figure 3 shows the microscope image of the sample surface after single grain scratching at a cutting speed of 10 m/s. A Nanofocus  $\mu\text{Scan}$  system was used to analyze the surface topography and determine scratch lengths ranging from 1.7 - 2.2 mm. The scratch width is 0.19 mm on average. By tilting the sample, a maximum scratch depth of  $4.8 \mu\text{m}$  was achieved. Larger depths of cut could not be reached despite the tilt angle of the sample. Possible causes are the grain retention force and the elasticity of the bond layer.



#### Process: Axial single grit scratching

material: Tigr T10Mg  
 abrasive grain: Diamond D 181  
 cutting speed:  $v_c = 10 \text{ m/s}$   
 feed (axial):  $v_f = 1486 \text{ mm/min}$   
 sample tilt:  $0.1^\circ$   
 tool diameter:  $D = 128 \text{ mm}$

Wie/115480 © IFW

Figure 3. Single grain geometry and tangential force analysis

A tangential force of 22.7 N already causes the grain to break out of the Cr-Cu bond. In the next step the geometric information of the individual scratches is correlated with the data of the force measurement to calculate the single grain grinding power. In the lower part of Figure 3, the tangential

force  $F_t$  (y-axis) is shown as a function of the maximum undeformed chip-cross-section  $A_{cu,max}$  (x-axis).  $K_c$  describes the slope of the linear relationship between the tangential force and the chip-cross-section. The dashed lines show the 95 % confidence interval of the fit function. Table 1 shows the empirically determined coefficients  $K_c$  at different cutting speeds. With an average RMSE of 1.421 N, the model provides a sufficiently accurate description of tangential force to calculate the single grain grinding power.

Table 1. Empirically determined coefficient  $K_c$ .

Cutting speed $v_c$ (m/s)	$K_c$ (-)	RMSE (N)
5	0.03307	1.0134
10	0.03199	1.9263
20	0.02191	1.3238

### 3.3 Simulation study

To investigate the fluid flow and temperature distribution near the grinding tool surface, a 2D implementation of the models (CM eqs. (1-4), DM eqs. (1-3, 5)) from Section 2.1 is done in FEniCS [16]. A small area of  $1000 \mu\text{m} \times 900 \mu\text{m}$  around the interface between free fluid and porous grinding tool is considered, with grains at the grinding surface (microscale model) and without (mesoscale). For the calculation of the supplied heat, the approach described in Section 2.2 is used to estimate the single grain grinding power. Figure 4 gives an overview of the respective input and output parameters of the simulation.

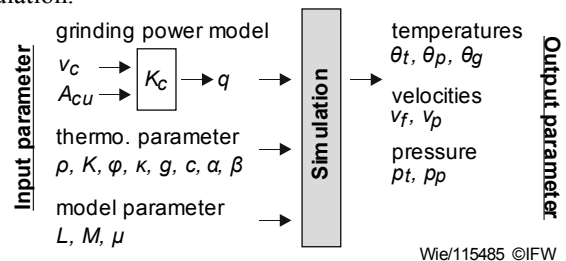


Figure 4. Input/output parameter of the thermo-fluid dynamic simulation

The same cutting speed ( $v_c = 10 \text{ m/s}$ ) as in the experiments is used for the simulation study. Since the majority of the heat is transferred to the workpiece [17], the heat transfer to the coolant and the grinding tool is initially assumed to be 15 % of the total heat flux. Further investigations aim to achieve a more precise identification of the distribution factors  $R_i$  in equation (7). While the single grain scratching experiments represent the heat production without the use of cooling lubricant, the simulation study considers fluid dynamics. The cooling lubricant is supplied from the left side, while the grinding surface is considered stationary (in a moving coordinate system, e.g.). For the fluid, a relative inflow velocity, at the left boundary, of  $v_f = 5 \text{ m/s}$  is assumed, resulting from a cutting speed of 10 m/s and coolant velocity of 15 m/s. In a real grinding process, a grain would only temporarily be in contact with the workpiece and coolant. Solely in this short time frame the heat source and coolant would affect the grain. However, the continuous grinding processes can be simplified by viewing it as stationary, where the individual grains are continuously heated by the grinding contact and cooled by new lubricant.

Figure 5 shows the temperature distribution for a single grain simulation, where the heat source in the grain corresponds to the single grain scratching experiments. In this first simulation study only the contact area without the workpiece is observed, immediately after the grain has performed a cut. The color depicts the temperature difference in Kelvin to the initial coolant temperature. With the discontinuous temperature model (DM), there is less heat flux into the fluid and the porous region due to the weakened heat exchange and thus the temperature of the grain is higher. Additionally, a sudden increase in temperatures at the interface between free fluid and porous region is clearly visible. In further experiments, temperature measurements will be conducted to identify the heat distribution factors and model parameters like heat exchange coefficients during the cutting process.

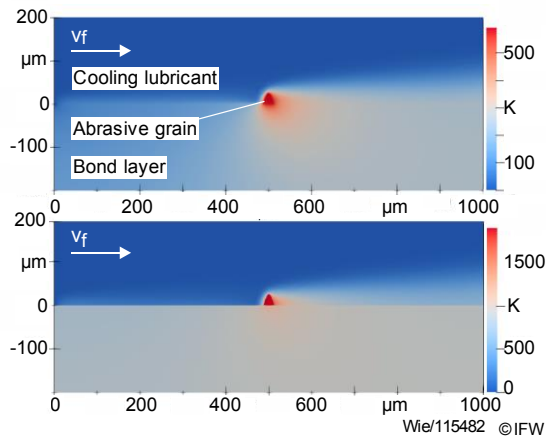


Figure 5. Temperatures from single grain microscopic simulation. Top: CM temperature, Bottom: DM temperature model.

To approximate the effective behavior for this situation, microscale simulations were performed with a varying number of (periodically arranged) identical grains. A comparison of the different temperature models is given in Figure 6. In this simulation, the overall heat source from single grain scratching experiments was equally distributed to all grains. This is motivated by the fact that in a continuous grinding process, the contact and material removal of individual grains is variable, depending on the grain orientation and distance between bond layer and grain tip. The total heat distributes over several grains participating in the cutting process. The 2D model with successive grains used here is an approximation of the real 3D situation, where grains are stochastically distributed across the surface of the grinding tool. Further investigations are planned to identify the actual heat distribution over multiple grains.

Finally, Figure 7 shows simulations with the effective mesoscale models with continuous (CM) and discontinuous (DM) temperature fields.

The fluid fields (not shown in Figure 7) are similar for both model variants and mostly depend on the values of the effective parameters from the mesoscale. The temperature models lead to different approximations of the results. The effective continuous model (CM) produces a similar profile, but contains less heat energy. The discontinuous model (DM) on the other hand can better approximate the energy of the system, but has the disadvantage of additional unknown parameters.

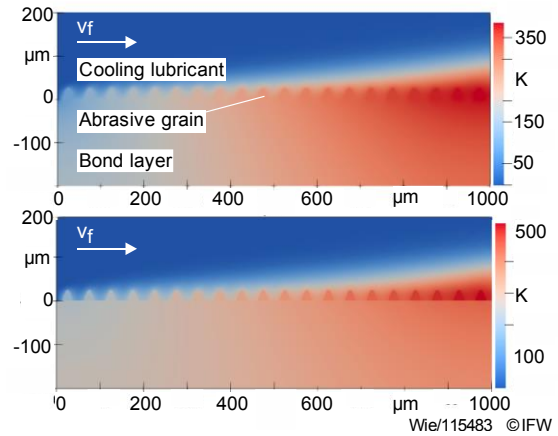


Figure 6. Temperatures from a 20-grain microscale simulation with CM (top) and DM (bottom) temperature.

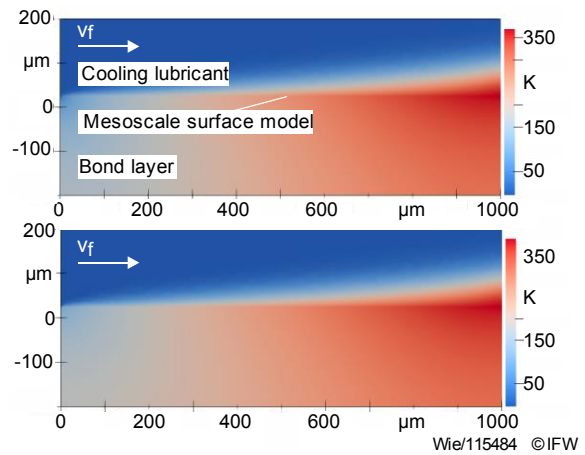


Figure 7. Temperatures from mesoscale simulation with CM (top) and DM (bottom) effective temperature.

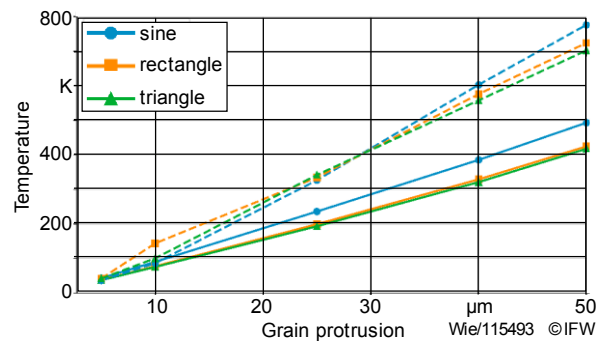


Figure 8: Temp. in grinding wheel 200  $\mu\text{m}$  below interface (continuous). Temp in fluid 20  $\mu\text{m}$  above interface (dashed)

Lastly, Figure 8 shows the temperature at two locations for different grain heights and geometries. Compared are the simulations for one single rectangular, triangular and sinusoidal grain. The heat production is scaled with the height of the grain, similar to equation (8), but not with the shape (e.g. quadratic and sinusoidal grain produce the same amount of heat). This enables a simpler comparison. For all considered geometries, the temperature increases approximately linearly with the grain height. The three grain structures lead to different fluid interactions and thus varying temperature fields.

#### 4. Conclusion and outlook

Tool grinding is an essential process step in the production of cemented carbide tools. Due to high material removal rates and subsequently high temperatures, especially in flue grinding, effective cooling of the workpiece and grinding tool is of great importance. To obtain a better understanding of thermomechanical effects, it is necessary to consider multiple scales. This paper presents methods for modeling process temperatures at the grinding tool including fluid dynamical effects of the cooling lubricant on the micro- and mesoscale as well as the underlying porous structure of the grinding tool. To determine the amount of heat generated during the grinding process, single grain scratching experiments were conducted. The results show a linear relationship between the tangential force and the single grain chip-cross-section. In combination with the cutting speed, the grinding power can be calculated, which corresponds to the total heat flux of a single grain. Further experiments are planned to transfer the approach to larger chip-cross-sections, different grain sizes, as well as to a process with the engagement of multiple grains. In addition, the influence of different cooling lubricants on the heat generation at single grains has to be investigated in future studies. The simulation results demonstrate the abilities of the developed multi-scale heat exchange models. The numerical model serves as a basis for future identification of relevant parameters, through comparison with experimental data. This applies on the one hand to the determination of local heat sources, their variations and their distribution to the bond layer, cooling lubricant and workpiece. On the other hand, to parameters like heat exchange and slip coefficients, and finally the selection of the best fitting model variants. This includes the porous structure of a grinding tool bond layer and fluid flow in the bonding. The focus of the simulations presented here was the fluid and temperature behavior at the grinding wheel. The interaction with the workpiece will be included in further models. Due to the general non-porous structure of the workpiece, the heat exchange model has only to account for rough surface structures due to the material abrasion. Additionally, the temporal engagement between coolant, grains and workpiece has to be considered in more detail (e.g. through time averaging).

#### Acknowledgments

This research was funded by the Deutsche Forschungsgemeinschaft (DFG, German Research Foundation) – project nr. 439916647 – as part of the Priority Program 2231 “Efficient cooling, lubrication and transportation – coupled mechanical and fluid-dynamical simulation methods for efficient production processes (FLUSIMPRO)”

#### References

[1] Pang, J., Li, B., Liu, Y., and Wu, C. 2016. Heat Flux Distribution Model in the Cylindrical Grinding Contact

- Area. *Procedia Manufacturing* 5, 158–169.
- [2] Meyer, D., Schumski, L., Guba, N., Espenhahn, B., and Hüsemann, T. 2022. Relevance of the region of interaction between the tool and the metalworking fluid for the cooling effect in grinding. *CIRP Annals* 71, 1, 301–304.
- [3] Wegener, K., Bleicher, F., Krajnik, P., Hoffmeister, H.-W., and Brecher, C. 2017. Recent developments in grinding machines. *CIRP Annals* 66, 2, 779–802.
- [4] Laciš, U., Pasche, S., Baheri. 2020. Transfer of mass and momentum at rough and porous surfaces. *J. Fluid Mech.* 884, A21 (2020.), 33.
- [5] Bergs, T., Röttger, J., Barth, S., and Prinz, S. 2021. Approach to the numerical modelling of the chip temperatures in single grain scratching. *Prod. Eng. Res. Devel.* 15, 3-4, 451–455.
- [6] Dittrich, M.-A., Denkena, B., and Wichmann, M. 2021. Parametric grinding wheel model for material removal simulation of tool grinding processes. *Procedia CIRP* 102, 381–386.
- [7] Beavers, G. S., Joseph, D. D. 1967. Boundary conditions at a naturally permeable wall. *J. Fluid Mech.*, 30 (1), 197–207.
- [8] Jäger, W., Mikelic, A. 2009. Modeling effective interface laws for transport phenomena between an unconfined fluid and a porous medium using homogenization. *Transp. Porous Media*, 78, 489–508.
- [9] Ochoa-Tapia, J.A., Whitaker, S. 1997. Heat transfer at the boundary between a porous medium and a homogeneous fluid. *Int. J. Heat Mass Transf.*, 40 (11), 2691–2707.
- [10] Rowe, W. B. 2017. Temperatures in Grinding—A Review. *Journal of Manufacturing Science and Engineering* 139, 12.
- [11] Ortega, N., Bravo, H., Pombo, I., Sánchez, J. A., and Vidal, G. 2015. Thermal Analysis of Creep Feed Grinding. *Procedia Engineering* 132, 1061–1068.
- [12] Aslan, D. and Budak, E. 2014. Semi-analytical Force Model for Grinding Operations. *Procedia CIRP* 14, 7–12.
- [13] Anderson, D., Warkentin, A., and Bauer, R. 2011. Experimental and numerical investigations of single abrasive-grain cutting. *International Journal of Machine Tools and Manufacture* 51, 12, 898–910.
- [14] Tawakoli, T., Kitzig, H., and Lohner, R. D. 2013. Experimental Investigation of Material Removal Mechanism in Grinding of Alumina by Single Grain Scratch Test. *AMR* 797, 96–102.
- [15] Öpöz, T. T. and Chen, X. 2012. Experimental investigation of material removal mechanism in single grit grinding. *International Journal of Machine Tools and Manufacture* 63, 32–40.
- [16] Alnaes, M. S., Blechta, J., Hake, J., Johansson, A., Kehlet, B., Logg, A., Richardson, C., Ring, J., Rognes, M. E., and Wells, G. N. 2015. The FEniCS Project Version 1.5. *Archive of Numerical Software* 3.
- [17] Rowe, W. B. and Jin, T. 2001. Temperatures in High Efficiency Deep Grinding (HEDG). *CIRP Annals* 50, 1, 205–208.